

Exfoliate apricot kernels, natural low-cost bio-sorbent for rapid and efficient adsorption of CN^- ions from aqueous solutions. Isotherm, kinetic and thermodynamic models

Mohammed Jaafar Ali Alatabe*, Mohammed Ali Rashid Hameed

Department of Environmental Engineering, College of Engineering, Mustansiriyah University, Baghdad, Iraq

ABSTRACT

Exfoliate apricot kernels were collected and prepared for adsorbing the cyanide ions from the aqueous solution. Fourier transforms infrared spectroscopy (FT-IR) and X-ray diffraction (XRD) and scanning electron microscopic (SEM) were utilized to describe the exfoliate apricot kernels. The adsorption experiments carried out were in a batch experiment, prepared 100 mL of cyanide solution for various temperature, pH, contact time, speed of mixer and dose of the adsorbent. The isotherms models were checked Langmuir, Freundlich, Temkin, and Harkins-Henderson, isotherm models. The isotherm coefficient of Langmuir, Freundlich, Temkin, and Harkins-Henderson models were 0.99, 0.8, 0.95 and 0.68 respectively. The Langmuir isotherm model best fitted for adsorption more than other models. The kinetic were studies pseudo-first-order, pseudo-second-order, intra particle diffusion, and Elovich kinetic models. The kinetic (R^2) constant for pseudo-first-order, pseudo-second-order, intra particle diffusion, and Elovich were 0.989, 0.947, 0.969 and 0.905 respectively. Pseudo-first-order giving a better fit for the process.

Keywords: Cyanide ions, Exfoliate apricot kernels, Natural low-cost bio-sorbent, Models.

OPEN ACCESS

Received: February 26, 2020

Revised: April 15, 2021

Accepted: April 28, 2021

Corresponding Author:
Mohammed Jaafar Ali Alatabe
jjaffer55@yahoo.com

 **Copyright:** The Author(s). This is an open access article distributed under the terms of the [Creative Commons Attribution License \(CC BY 4.0\)](https://creativecommons.org/licenses/by/4.0/), which permits unrestricted distribution provided the original author and source are cited.

Publisher:
[Chaoyang University of Technology](https://www.caejournal.com/)
ISSN: 1727-2394 (Print)
ISSN: 1727-7841 (Online)

1. INTRODUCTION

Industrial activities can generate significant loads of pollutants that are released into water sources. Gold mining uses highly toxic compounds such as cyanide which is considered potentially lethal to any ecosystem (Dash et al., 2009). In contact with water, it produces hydrocyanic acid, a compound that causes serious illnesses in humans and animals, and degradation of soil fertility. The use of cyanide in gold mining is an important cause of biodiversity depletion in developing countries. The term cyanide refers to a singularly charged anion consisting of one carbon atom and one nitrogen atom joined with a triple bond, CN^- . The most toxic form of cyanide is free cyanide, which includes the cyanide anion itself and hydrogen cyanide, HCN, either in a gaseous or aqueous state. At a pH of 9.3 - 9.5, CN^- and HCN are in equilibrium, with equal amounts of each present. At a pH of 11, over 99% of the cyanide remains in solution as CN^- , while at pH 7, over 99% of the cyanide will exist as HCN. Although HCN is highly soluble in water, its solubility decreases with increased temperature and under highly saline conditions. Both HCN gas and liquid are colorless and have the odor of bitter almonds, although not all individuals can detect the odor (Akcil, 2010; Donato et al., 2017).

Cyanide is one of the anthropogenic contaminants in natural water through several industrial effluents and considered highly toxic for aquatic life and human beings (Paschka et al., 1999). It enters the human body through inhalation, ingestion, absorption through the skin, eyes, and mucous membranes. Industrial exposure even in short term can cause tremors and neurological disorders, while long-term exposure causes weight loss, thyroid dysfunction and nerve damage, and hypoxia (Kulig and Ballantyne, 1991).

Exposure to cyanide from inhalation through showering and absorption through the skin in bathing is not normally expected to be significant (Brüger et al., 2018). Cyanide is certainly a chemical that is toxic and lethal to humans if ingested (Paschka et al., 1999; Kulig and Ballantyne, 1991). This is likely why its use by the mining industry often instills fear, anger, and opposition by both the communities near the mine and the environmental community (Brüger et al., 2018; Dunbar and Heintz, 1997).

Human industrial activities which lead to the generation of large quantities of wastewater has been on the increase, especially wastewater generated from local food processing industries (cassava processing mills) which have become an environmental challenge in developing countries where the processing of staple foods such as cassava is encouraged to provide both food and employment opportunities for the increasing populace (Behnamfard and Salarirad, 2009; Eletta et al., 2016). The processes involved in starch production from cassava and other allied products such as gari and fufu leads to the release of large quantities of naturally occurring cyanoglycosides compounds present in cassava (Kaewkannetra et al., 2009).

As pressure increases for control of toxic waters, interest in new methods of treatment also increases. The detoxification of cyanide-bearing wastes is one area that has received particular attention. Both physical and chemical methods of removing cyanide from water are feasible and include precipitation (Xie and Wang, 2017), foam separation (Dai et al., 2012), ion exchange (Meenakshi and Viswanathan, 2007; Kurama and Çatalarik, 2000) air purging (Parga et al., 2003), electrolytic (Dai et al., 2010). Lots of methods have been used to deal with cyanide and precious metals (Dai et al., 2010). These methods are mainly divided into two kinds, the destruction of cyanide in its effluents and the recovery of cyanide (Lu et al., 2015). Electrochemistry method (Dai et al., 2010), chlorine and H₂O₂ oxidation process (Sun et al., 2014), SO₂-air oxidation process (Parga et al., 2003), destruction of cyanide by biological treatment methods (Sheremata and Hawari, 2000; Sarma et al., 2019).

Many papers mainly discuss several factors for the adsorption performance of the resins such as adsorption capacity, resin amount, time, temperature. Also, the adsorption thermodynamics and kinetics were analyzed (Sarma et al., 2019). Developments in the field of low-cost adsorbents have led to an interest in their use in water treatment processing (Eletta et al., 2016). Sorbents may be either natural, based on plants or minerals raw and oxidized coke (Hattab et al., 2016), activated carbon surface (Behnamfard and Salarirad, 2009; Dai et al., 2010; Ibragimova et al., 2013) granular activated carbon (Guo et al., 1993; Aliprandini et al., 2020), carbon-micro silica composite (Zhang et al., 2012), two different bio-adsorbents (Dwivedi et al., 2016), coffee husk (Gebresemati et al., 2018), magnetic hydroxyapatite nanoparticles (Nourozi et al., 2015), copper and nickel-impregnated powder activated

carbon and clay (Mbadcam et al., 2009; Alatabe, 2018), mesoporous zeolite modified by cetyltrimethyl-ammonium bromide surfactant (Papari et al., 2017), calcinated eggshells (Eletta et al., 2016).

There are two different types of exfoliants: chemical and mechanical, both can be a result of natural ingredients. Certain ingredients may work as a chemical exfoliant due to their acidity or the presence of certain enzymes that will aid in removing dead skin cells without a physical component. A more commonly understood exfoliator is mechanical exfoliants. These utilize microbeads, granules, or other natural materials, such as apricot seed powder, to aid in physically removing dead and damaged skin cells (Zhang, et al., 2019). Exfoliate apricot kernels used as an adsorbent by removal methylene blue from aqueous solutions (Namal and Kalipci, 2020), removal of Cr (VI) (Kalipci and Namal, 2018), removal of malachite green (Abbas, 2020), production carbonaceous adsorbents from apricot kernels (Krasilnikova et al., 2005).

In the present work, exfoliate apricot kernels a novel and natural plant adsorbent, examined for the removal of CN⁻ ions from aqueous solutions, as adsorbent under several conditions like temperature, adsorbent dose, contact time, and pH, finding a general equation relating these conditions to give its optimum value and studying the adsorption isotherm, kinetics and thermodynamic.

2. MATERIALS AND METHODS

2.1 Exfoliate Apricot Kernels

Apricot stone shells mostly consist of lignocellulose material, i.e. of insoluble fibers. Hence, they are a wood-like, inflammable raw material with a characteristic light brown color and a high calorific value. In a dry state, they are extremely durable and their mechanical strength/hardness is similar to olive stone granules.

2.2 Surface Characterization of Exfoliate Apricot Kernels

Exfoliate apricot kernels were collected as a low-cost bio-adsorption waste (were collected from local markets), exfoliate apricot kernels were eliminated from the fruit and were milled to a fine powder into 100-200 µm mesh size to use in experiments, by a hammer mill (Fitzmill Mill Hammer, L1A, R24330, China), Fig.1 represents the preparation steps of exfoliate apricot kernels to experimental work. Then, weighed the powder of exfoliator apricot kernels with a sensitive balance of 0.00001 accuracies to prepared for the experiments. The product from milling was dried in an oven at 105°C for 24 h. To avoid further moisture absorption, samples were preserved in desiccators. Dried samples were then taken in a porcelain crucible and covered with a lid to be placed in a control muffle furnace at 150°C for an hour, to get dried powder.



Fig. 1. Preparation steps of exfoliate apricot kernels to experimental work

The samples were washed with 1M hydrochloric acid solutions firstly, and then with distilled water until the pH value reached 7.0. After washing, the samples were dried in an oven at 105°C for 24 h. Then the dried samples were preserved in desiccators to avoid further moisture absorption. The adsorbent showed a fluffy, highly porous, and rough microstructure, containing some voids and cracks which were suitable for the CN⁻ ions adsorption. The properties of exfoliate apricot kernels samples were tested by several techniques:

- The functional groups were specified by FT-IR (Shimadzu 8400S FTIR spectrometer, equipped with KBr beam splitter) using approximately 5 mg of each sample along with 5 mg KBr. FT-IR spectrophotometer was operated at a spectral range of 4000–400 cm⁻¹ with a maximum resolution of 0.5 ~ 0.85 cm⁻¹.
- Energy dispersive X-ray (EDX) spectroscopy allows elemental identification by measuring the number and energy of X-rays emitted from a specimen after excitation with an electron beam, (Shimadzu device, EDX-7000) it was used for the detection of the elements in the samples (qualitative analysis).
- The morphology of the sample was evaluated using an Em-Craft (Korea): Table-top scanning electron microscope (SEM Cube-1000). Samples were dehydrated by putting them into critical point drying equipment or freeze-dried. The exfoliate apricot kernels powder was fixed in an aluminum plate (specimen holder), using an electrically conductive tap and a coating of gold at 10 mbar for 90 s was applied. Each sample was transferred to the microscope for observation. The procedure was applied to gain information about the arrangements of particles that correlated with the structure of samples.

2.3 Chemical Reagents

Cyanide solution was prepared by dissolving sodium cyanide in double distilled water to yield a stock solution containing 1 mg (CN⁻)/mL. For prepared the required concentration samples, diluting the stock solution used in experiments. Utilizing 1M NaOH or 1 M H₂SO₄ for adjusted the pH of the experimental solutions. The chemicals utilized were of analytical grade.

2.4 Procedure

Firstly, 100 mL of prepared solution contain CN⁻ ions was used to study the ability of exfoliate apricot kernels to

adsorb CN⁻ ions from solution. The factors investigated were, the dose of adsorbent (1, 5, 10 and 50 g) and shaker with a perforated platform, Tablar 2000, Heidolph for mixing the exfoliate apricot kernels, temperature (25, 35, 45 and 55°C) (With heating plate, magnetic stirrer and thermostat to control the heating and mixing solution, also used (water bath) model WNB from Memmert company for heated and controlling the process temperature), the contact time (10, 40, 60 and 90 min.) and pH of the solution (2, 4, 6 and 7). The rotational speed of the mixer was (200 rpm). The adsorption process of CN⁻ ions needs statistical analysis for the experimental gotten data to develop an optimal adsorption model.

The adsorption capacity q was calculated from the difference between the initial concentration and equilibrium adsorbate compound concentration, which is as follows the equation:

$$q = \frac{V(C_0 - C_e)}{M} \quad (1)$$

Where q is the adsorption capacity (mg/g), C_0 and C_e are the initial and equilibrium concentration (mg/L), respectively, M is the adsorbent dosage (g) and V is the solution volume (L). The CN⁻ ions removal percentage can be calculated as follows:

$$\text{CN}^- \text{ ions (\% Removal)} = \frac{C_0 - C_e}{C_0} \times 100 \quad (2)$$

3. RESULTS AND DISCUSSION

The properties of the exfoliate apricot kernels were examined using FT-IR, EDX, and SEM.

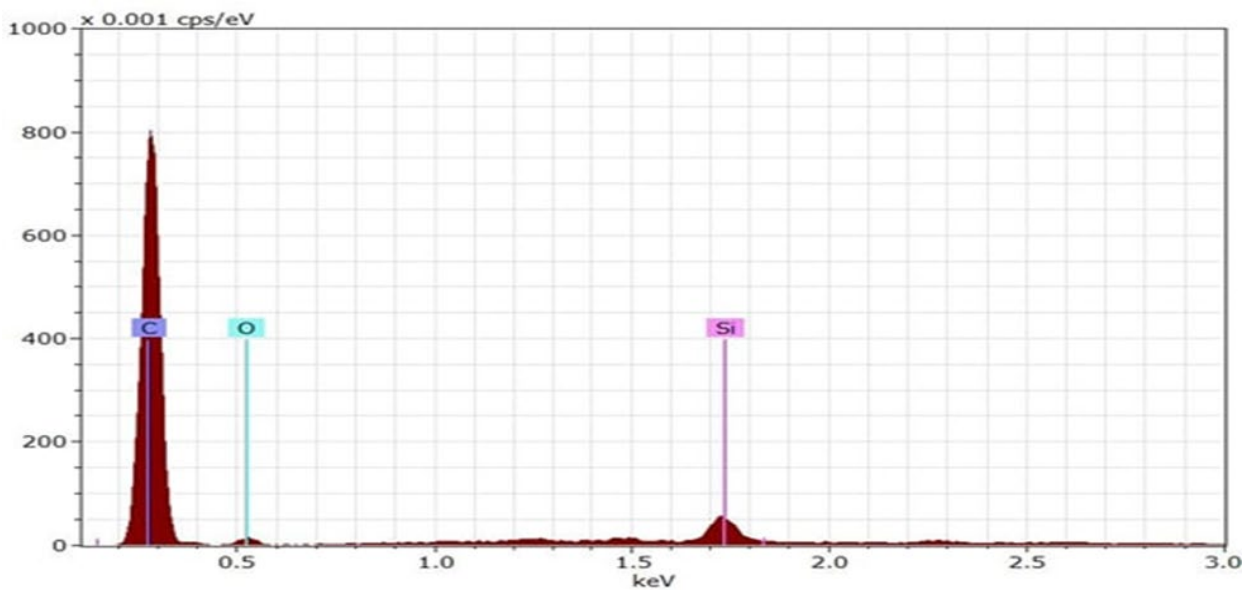
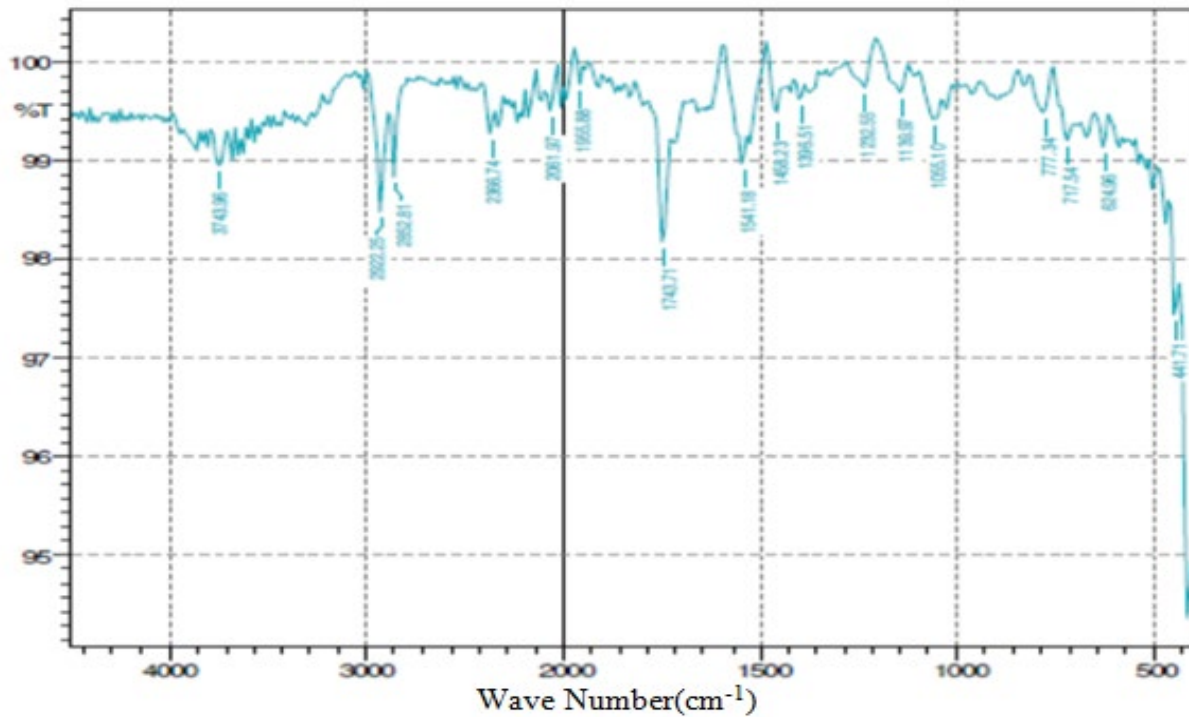
3.1 Fourier Transforms Infrared Spectroscopy (FT-IR) and EDX Spectra Investigation

FT-IR spectroscopy has been utilized to test the structural dynamics, structural composition, conformational changes (effect of binding, temperature, and pH), structural stability, and aggregation of proteins. It has been used to identify functional group of compounds, such as carbohydrates and esters, as well as inter atom chemical bonds in a variety of samples. The FT-IR spectra of exfoliate apricot kernels were indistinguishable in the wavenumber range of 4000–400 cm⁻¹, only with subtle differences in the intensity of bands/peaks. Infrared spectra of exfoliate apricot kernels indicated by the presence of narrow peak bands at 1743.71 cm⁻¹ attributes to aldehyde and ketone C = O stretching. The position of the C = O stretching indicated the hydrogen

bonding and conjugation within the molecules. High intense peaks followed by a peak at 2922.25 cm^{-1} and 2852.81 cm^{-1} , attributed to O-H stretching (carboxylic acid) vibrations and aldehyde C-H stretching. These O-H stretching vibrations may be due to carboxylic compounds in the polymer protein matrix. The carboxylic acids

(RCOOH) exist as a dimer, except in dilution solution, due to strong intermolecular hydrogen bonding (Fig. 2A).

The EDX spectra gave an interesting finding. EDX is a very useful tool for identifying elements on the adsorbent surface. The presence of C, O, and Si, ions on the exfoliate apricot kernels surface were confirmed by the peaks at 0.32, 0.6, and 2.2 keV, respectively (Fig. 2B).



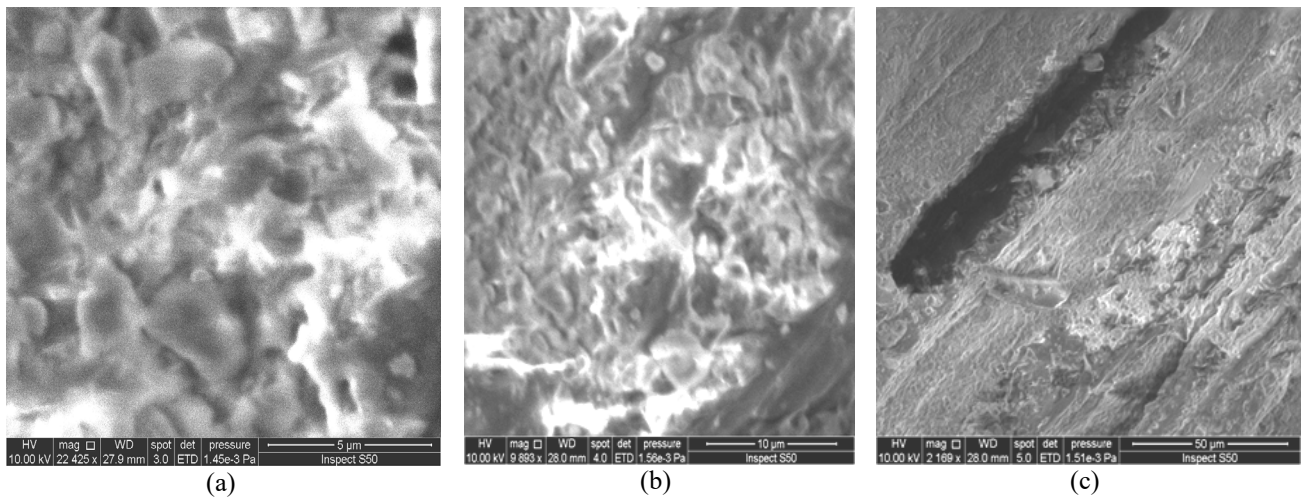


Fig. 3. Scanning electron microscopic (SEM) of exfoliate apricot kernels

3.2 Scanning Electron Microscopic (SEM)

Investigations

The scanning electron microscope (SEM) is one of the most versatile methods for the examination and analysis of the microstructure, chemical composition, and physical (size and shape) characterizations. It shows the arrangement of starch granules and the protein network in the matrix. The SEM was conducted at a magnification of 1000 x and 1200x. The images (A, B and C) in Fig. 3 for the exfoliate apricot kernels press cake reveals that the press cake had some polygonal and irregular shapes representing the presence of starch molecules in the sample. Whereas, some cracked surfaces represented the presence of protein. Starch granules seem to be surrounded by little pieces of other protein material, giving the appearance of rousing dust in exfoliate apricot kernels press cake. The differences in the picture were the variations in the number of individual granules and compound granules or may be due to different processing conditions and extraction methods to form different structural aggregate. The results of SEM tests are at the bottom of each image.

3.2.1 Effect of pH

Cyanide is very reactive, forming simple salts with alkali earth cations and ionic complexes of varying strengths with numerous metal cations; the stability of these salts is dependent on the cation and pH. The salts of sodium, potassium and calcium cyanide are quite toxic, as they are highly soluble in water, and thus readily dissolve to form free cyanide. Operations typically receive cyanide as solid or dissolved NaCN or Ca(CN)₂. Weak or moderately stable complexes such as cadmium, copper, and zinc are classified as weak-acid dissociable (WAD). Although metal-cyanide complexes by themselves are much less toxic than free cyanide, their dissociation releases free cyanide as well as the metal cation which can also be toxic. Even in the neutral pH range of most surface water, WAD metal-cyanide

complexes can dissociate sufficiently to be environmentally harmful if in high enough concentrations.

Generally, changes of pH were effect by the metal ion's adsorption, due to the activity of protons and ions. Fig. 4 represented the pH changes effect on the CN⁻ ions adsorption by exfoliate apricot kernels as adsorbent material, test results were showing that the solution pH changing affected slightly on the CN⁻ ions adsorption. When pH = 4 the CN⁻ ions uptake 98.8% increased slightly, then pH < 4 decreases slightly. When the solution pH between 6.5 to 7, the adsorption relatively percentage was constant between 98.8% to 99%, but at pH = 7 the adsorption efficiency decreasing to less than 95% because the CN⁻ ions started to precipitate.

Cyanide forms complexes with gold, mercury, cobalt, and iron that are very stable even under mildly acidic conditions. However, both ferro- and ferri-cyanides decompose to release free cyanide when exposed to direct ultraviolet light in aqueous solutions. This decomposition process is reversed in the dark. The stability of cyanide salts and complexes is pH-dependent, and therefore, their potential environmental impacts and interactions (i.e. their acute or chronic effects, attenuation, and re-release) can be varied.

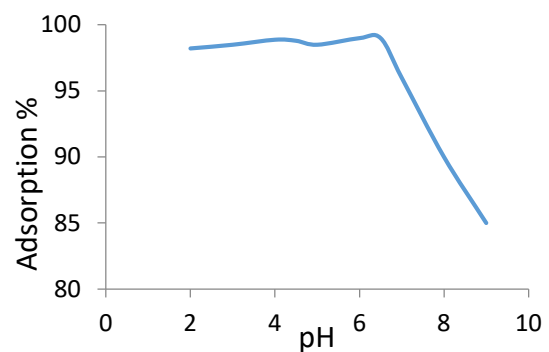


Fig. 4. pH changes effect on CN⁻ ions adsorption efficiency onto exfoliate apricot kernels

3.2.2 Effect of Temperature

The effect of temperature on the CN⁻ ions removal was shown in Fig. 5. When the system temperature went up, the solubility of the CN⁻ ions in wastewater increased correspondingly, removal of CN⁻ ions would increase at pH 7, over 99% of the cyanide will exist as HCN. Although HCN is highly soluble in water, its solubility decreases with increased temperature and under highly saline conditions.

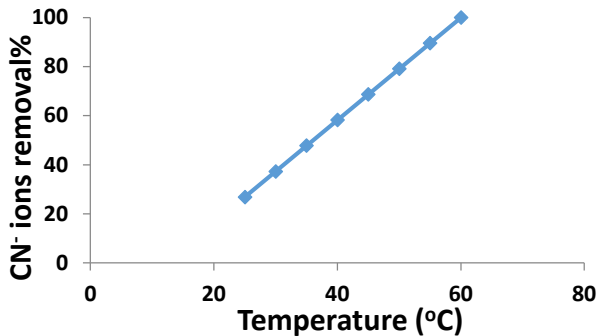


Fig. 5. The effect of temperature on CN⁻ ions removal at adsorbent dose = 5 gm/100 mL, t = 60 min

3.2.3 Effect of Adsorbent Dose

The effect of adsorbent dosage on the percentage removal of CN⁻ ions is depicted in Fig. 6 at specific conditions. It can be seen that the removal of CN⁻ ions increased with increasing adsorbent dosage and attained a maximum value (100%) at an adsorbent dosage of 0.95 gm/100 mL. The phenomenon is associated with an increase in available binding sites for adsorption in higher sorbent dosage, but sorption capacity decreases with an increase in sorbent dosage.

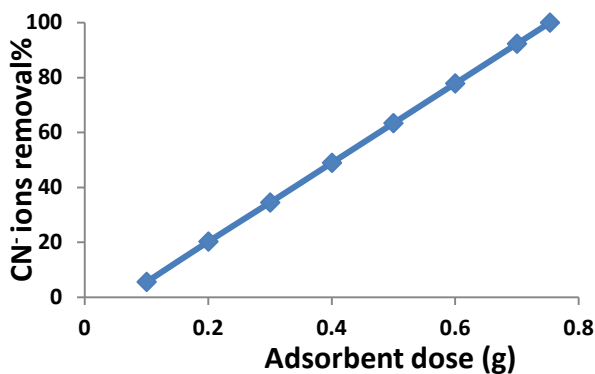


Fig. 6. The effect of adsorbent dose on CN⁻ ions removal at t = 60 min, T = 45°C

3.2.4 Effect of Contact Time

The relationship between contact time and CN⁻ ions removal by exfoliate apricot kernels was conducted through batch experiments to achieve the equilibrium as shown in Fig. 7. The CN⁻ ions removal increased with contact time. The rapid adsorption in the first 5 to 30 minutes can be attributed to the increased availability of vacant surface sites

at the initial stages. The optimal contact time was 60 minutes. The adsorption rapidly occurs and is normally controlled by the diffusion process from the bulk to the surface.

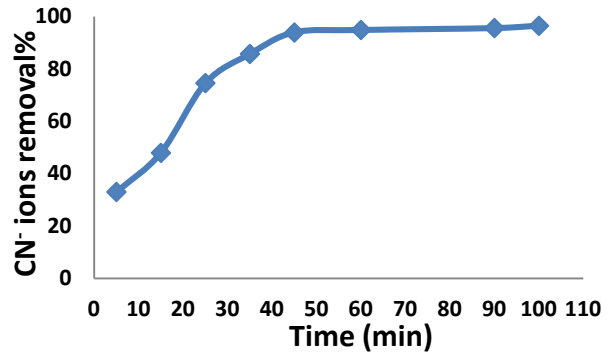


Fig. 7. The effect of contact time on CN⁻ ions removal by exfoliate apricot kernels at adsorbent dose = 5 gm/100 mL, T = 45°C

3.3 Adsorption Isotherms Models

Adsorption isotherms are mathematical models that describe the distribution of the adsorbate species among liquid and solid phases, based on a set of an assumption that is related to the heterogeneity/ homogeneity of the solid surface, the type of coverage, and the possibility of interaction between the adsorbate species (Hattab et al., 2016; Jaafar and Alatabe, 2019).

3.3.1 The Langmuir Models

The Langmuir isotherm is based on the assumption that all the adsorption sites are energetically identical (monolayer adsorption) and adsorption occurs on a structurally homogeneous adsorbent (Langmuir, 1918). The Langmuir isotherm is given:

$$q_e = \frac{K_L C_e}{1 + a_L C_e} \quad (4)$$

where K_L (dm³/g) and a_L (dm³/mg) represent Langmuir constants (Langmuir, 1916; Langmuir, 1917).

3.3.2 The Freundlich Model

This isotherm is derived from the assumption that the adsorption sites are distributed exponentially to the heat of adsorption (Freundlich, 1906), and it is given by:

$$q_e = K_f C_e^{1/n} \quad (5)$$

Where q_e is the adsorbed metal ions (mg/g), C_e is CN⁻ ions concentration in the solution at equilibrium (mg/L), K_f (mg/g) indicates the multilayer adsorption capacity and n an empirical parameter related to the intensity of adsorption.

3.3.3 Temkin Isotherm Model

This model was obtained with consideration of adsorption interaction and adsorption substances (Hadi et al., 2020; Vadi et al., 2011; Vadi et al., 2010), which consider the effects of the heat of adsorption of all molecules in the

layer, would decrease linearly with coverage due to the adsorbate and adsorbent interactions and is given by:

$$q_e = \frac{RT}{b} \ln AC_e \quad (6)$$

Here $\left(\frac{RT}{b}\right) = B$ (J/mol), which is Temkin constant, A (l/g) is the equilibrium binding constant, R is the universal gas constant and $T(K)$ is absolute solution temperature.

3.3.4 Harkins-Henderson Model

This model explains multilayer adsorption and the existence of heterogeneous pore distribution in the adsorbent (Vadi et al., 2011; Vadi et al., 2010). The Harkins-Henderson isotherm has been applied in the following form:

$$q_e = \frac{K_{H-H}^{1/n}}{c_e^{1/n}} \quad (7)$$

n and K_{H-H} are isotherm constants.

From the above isotherm models the results were obtained, the linearized form of Langmuir, Freundlich, Temkin, and Harkins-Henderson isotherm models, using Equations (4) to (7) respectively, were analyzed using Microsoft Excel Software to find the isotherm constants. These constants presented in Table 1, it can be seen that the regression correlation coefficient (R^2) of the Langmuir equation ($R^2 = 0.998$) is more linear when compared with that of other equations, implying that the adsorption isotherm data are well fitted by the Langmuir isotherm. Fig. 8 shows the experimental curve and isotherm model curves.

The fact that the Langmuir isotherm fits the experimental data very well, the adsorption is single-layer and the maximum adsorption corresponds to a saturated monolayer of CN^- ions molecules on the exfoliate apricot kernels surface, the energy of adsorption is constant, and there is no transmigration of CN^- ions in the plane of the surface (Alatabe and Kariem, 2019). The Langmuir isotherm model is based on the assumption that there are a finite number of active sites that are homogeneously distributed over the surface of the adsorbent. These active sites have the same affinity for adsorption of a monomolecular layer and there

is no interaction between adsorbed molecules (Vadi et al., 2010; Alatabe and Kariem, 2019).

Table 1. The constants of isotherm models

Isotherms models	Parameters	Values
Langmuir	q_L	0.125
	K_L	1.14
	R^2	0.99
Freundlich	n	0.65
	K_f	1.67
Temkin	R^2	0.80
	B	0.88
	A	32.50
Harkins-Henderson	R^2	0.95
	n	1.229
Harkins-Henderson	K_{H-H}	2.15
	R^2	0.68

3.4 Adsorption Kinetics

The kinetics of adsorption describes the rate at which adsorbate is adsorbed on the adsorbent. The adsorption kinetics is required for selecting optimum operating conditions for the full-scale batch process. It is also helpful for the prediction of the adsorption rate, giving important information for designing and modeling the process. Several kinetic models are used to analyze adsorption kinetics data (Alatabe and Hussein, 2018).

3.4.1 Pseudo-First-Order Kinetic Model

This model proposed by Lagergren. The linearized form is shown in Equation (8).

$$\log (q_e - q_t) = \log q_e - k_1 t / 2.303 \quad (8)$$

q_e (mg/g) and q_t (mg/g) are adsorption capacity at equilibrium and at time t respectively. k_1 is the rate constant of pseudo first-order adsorption (min^{-1}) (Pan and Xing, 2010).

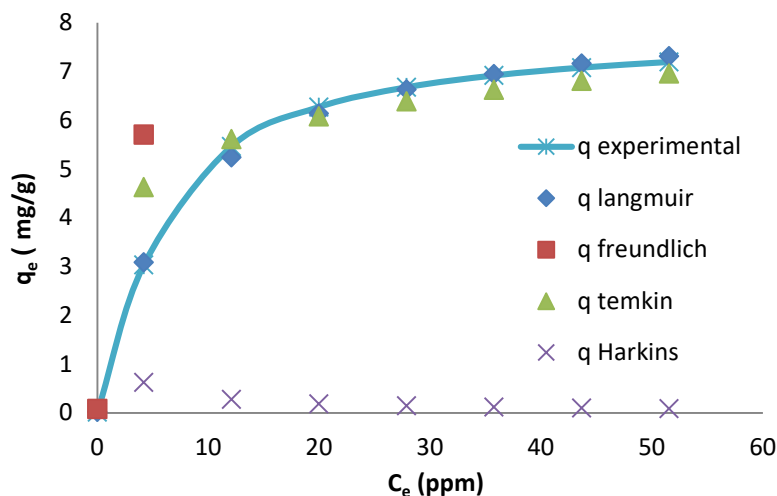


Fig. 8. Adsorption isotherm of CN^- ions adsorbed onto exfoliate apricot kernels

3.4.2 Pseudo-Second-Order Kinetic Model

The pseudo-second-order kinetic model can be represented as follows:

$$\frac{dq_t}{dt} = k_s(q_e - q_t)^2 \tag{9}$$

Where k_s is the rate constant of adsorption, $g/(mg \cdot min)$ (Ho and McKay, 1999; Ho, 2006).

3.4.3 Intra Particle Diffusion Study

In the batch mode adsorption process, initial adsorption occurs on the surface of the adsorbent. Also, the sorbate can diffuse into the interior pores of the adsorbent. Weber and Morris suggested the following kinetic model to investigate if the adsorption is intraparticle diffusion or not (Saleh et al., 2016; Simonin and Bouté, 2016). The relationship may be given as:

$$q_t = k_{id} t^{1/2} + C \tag{10}$$

Where k_{id} and C are the intra-particle diffusion rate constant.

3.4.4 Elovich Model

The Elovich equation was developed for describing the kinetics of heterogeneous chemisorption, the equation assumes a heterogeneous distribution of adsorption or activation energies that vary continuously with surface coverage and it's widely used in liquid-solid adsorption (Wu et al., 2009). The Elovich equation is generally expressed as:

$$q_t = 1/\beta \ln(\alpha\beta) + 1/\beta \ln t \tag{11}$$

Where, α is the initial bio-sorption rate ($mg/g \cdot min$) and β is related to the extent of surface coverage and the activation energy for chemisorption (g/mg).

From the above kinetic models, the results were obtained, the instantaneous adsorption of the batch process was investigated using four different models. These kinetic models included the pseudo-first-order, pseudo-second-order, intra-particle diffusion, and Elovich models (Cheung et al., 2000). The experimental results were employed to derive the kinetic parameters using these models.

Table 2. Kinetic models constants for the exfoliate apricot kernels adsorption

Model	Parameters	Values
Pseudo-first order Equation (8)	q_e	145.7
	k_1	0.0354
	R^2	0.989
Pseudo-Second order Equation (9)	q_e	0.635
	k_s	1.955
	R^2	0.947
Intra-Particle diffusion Equation (10)	k_{id}	0.945
	C	0.455
	R^2	0.969
Elovich Equation (11)	α	2.559
	β	0.487
	R^2	0.905

Table 2 shows the results of these analyses and Fig. 9 to 12 represent the adsorption capacity with the fitted model. Fig. 9 represents the relation of $\log(q_e - q_t)$ and time for pseudo-first-order model, Fig. 10 represents the relation of $(time/q_t)$ and time for pseudo-second-order model, Fig. 11 represents the relation of q_t and $(time)^{0.5}$ for the intra-particle diffusion model, and Fig. 12 represents the relation of q_t and $\ln(time)$ for Elovich model.

By comparing the correlation coefficient (R^2) values of each curve for all four models listed in Table 2, it seems that the kinetics of CN^- ions adsorption onto exfoliate apricot kernels was found to be fitted with a pseudo-first-order model more than other models.

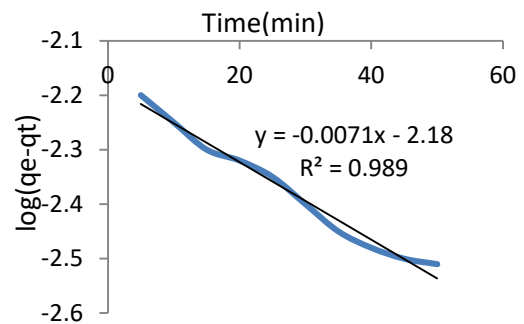


Fig. 9. Pseudo-first-order adsorption kinetics of CN^- ions onto exfoliate apricot kernels

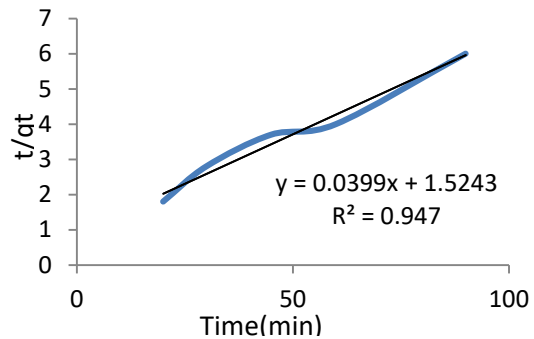


Fig. 10. Pseudo-second-order adsorption kinetics of CN^- ions onto exfoliate apricot kernels

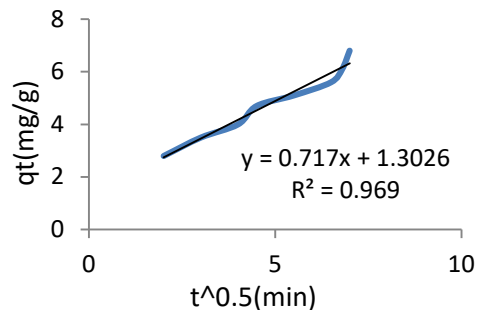


Fig. 11. Intra-particle adsorption kinetics of CN^- onto exfoliate apricot kernels

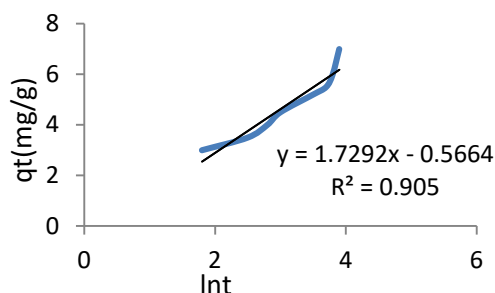


Fig. 12. Elovich model for adsorption kinetics of CN⁻ onto exfoliate apricot kernels

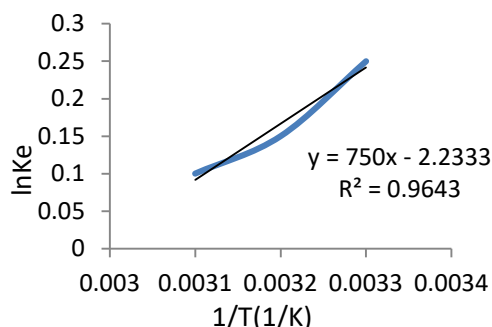


Fig. 13. Thermodynamic parameters for CN⁻ ions adsorption onto exfoliate apricot kernels

3.5 Adsorption Thermodynamic Results

The effect of CN⁻ adsorption on the temperature was studied at a temperature ranging from 20 to 60°C. The Gibbs energy change (ΔG°) indicates the degree of the spontaneity of an adsorption process, and a higher negative value reflects more energetically favorable adsorption (Hussein and Alatabe, 2019; Alatabe, 2018; Alatabe, 2018). Thermodynamic parameters such as standard free energy change (ΔG°) (Liu, 2009), standard enthalpy change (ΔH°) and standard entropy change (ΔS°) were calculated using the following relations :

$$\Delta G^\circ = -RT \ln K_c \quad (12)$$

$$\Delta G^\circ = \Delta H^\circ - T \Delta S^\circ \quad (13)$$

where R is the universal gas constant (8.314 J/mol. K), T is the temperature (K) and K_c is the thermodynamic equilibrium constant without units (Alatabe, 2018; Ho and Ofomaja, 2006). The enthalpy change (ΔH°) and entropy change (ΔS°) of adsorption are obtained from the following equation

$$\ln K_c = \frac{\Delta S^\circ}{R} - \frac{\Delta H^\circ}{RT} \quad (14)$$

According to Equation (14), ΔH° and ΔS° parameters can be calculated from the slope and intercept of a plot of $\ln K_c$ versus $1/T$, respectively (Fig. 13).

These thermodynamic parameters can offer insight into the type and mechanism of an adsorption process. Values of free energy change ΔG° are negative confirming that CN⁻ ions adsorption onto exfoliating apricot kernels is spontaneous and thermodynamically favorable since ΔG° became more negative (-0.27, -0.39, -0.55 and -0.63 kJ/mol) with an increase in temperature at 25, 35, 45 and 55°C respectively, indicating a high driving force and hence resulting in higher adsorption capacity at a higher temperature. The positive value of ΔH° indicated the endothermic adsorption process (0.756 kJ/mol). A little but positive value of ΔS° (0.0225 kJ/mol.K) in the temperature range 20–60°C suggested increased randomness at the solid-solution interface because some water molecules were dislodged during adsorption of CN⁻ ions.

4. CONCLUSIONS

The study showed that the exfoliate apricot kernels was effective in adsorption CN⁻ ions from wastewater due to the availability of effective functional groups as shown in FT-IR. 99% CN⁻ removal at temperature 45°C, pH 7, adsorbent dose 0.95 g/100 mL and 60min contact time. The Langmuir equation fits the experimental data for equilibrium isotherm of CN⁻ ions removal more than other equations. The pseudo-first-order adsorption is predominant for kinetics and thermodynamics studies. Finally, as the exfoliate apricot kernels were efficient in absorbing CN⁻ ions from the wastewater, we recommend using it in the treatment of wastewater contaminated with CN⁻ ions.

ACKNOWLEDGMENT

The authors are thankful for the technical support of the Environmental Engineering Department, Al-Mustansiriyah University for giving their investigative services.

CONFLICT OF INTERESTS

The authors would like to declare no conflict of interest in the publication of this manuscript.

REFERENCES

- Abbas, M. 2020. Experimental investigation of activated carbon prepared from apricot stones material (ASM) adsorbent for removal of malachite green (MG) from aqueous solution, *Adsorption Science & Technology*, 38, 24–45.
- Akcil, A. 2010. A new global approach of cyanide management: international cyanide management code for the manufacture, transport, and use of cyanide in the production of gold, *Mineral Processing & Extractive Metallurgy Review*, 31, 135–149.
- Alatabe, M. jaafar, 2018. Crystallization in phase change materials, *International Journal of Scientific Research in Science, Engineering and Technology*, 4, 93–99.

- Alatabe, M. jaafar, 2018. A novel approach for adsorption of copper (II) ions from wastewater using cane papyrus, *International Journal of Integrated Engineering*, 10, 96–102.
- Alatabe, M.J. 2018. Adsorption of copper (II) ions from aqueous solution onto activated carbon prepared from cane papyrus, *Pollution*, 4, 649–662. doi: DOI: 10.22059/poll.2018.249931.377.
- Alatabe, M.J.A., Hussein, A. 2018. Adsorption of nickel ions from aqueous solution using natural clay, *Al-Nahrain Journal for Engineering Sciences*, 21, 223–229.
- Alatabe, M.J.A., Kariem, N.O. 2019. Thorns, a novel natural plants for adsorption of lead (II) ions from wastewater equilibrium, isotherm, kinetics and thermodynamics, *Eurasian Journal of Analytical Chemistry*, 14, 163–174.
- Aliprandini, P., Veiga, M.M., Marshall, B.G., Scarazzato, T., Espinosa, D.C.R. 2020. Investigation of mercury cyanide adsorption from synthetic wastewater aqueous solution on granular activated carbon, *Journal of Water Process Engineering*, 34, 101154.
- Behnamfard, A., Salarirad, M.M. 2009. Equilibrium and kinetic studies on free cyanide adsorption from aqueous solution by activated carbon, *Journal of hazardous materials*, 170, 127–133.
- Brüger, A., Fafilek, G., Rojas-Mendoza, L. 2018. On the volatilisation and decomposition of cyanide contaminations from gold mining, *Science of the Total Environment*, 627, 1167–1173.
- Cheung, C.W., Porter, J.F., McKay, G. 2000. Elovich equation and modified second-order equation for sorption of cadmium ions onto bone char, *Journal of Chemical Technology & Biotechnology*, 75, 963–970.
- Dai, X., Breuer, P.L., Jeffrey, M.I. 2010. Comparison of activated carbon and ion-exchange resins in recovering copper from cyanide leach solutions, *Hydrometallurgy*, 101, 48–57.
- Dai, X., Jeffrey, M.I., Breuer, P.L. 2010. A mechanistic model of the equilibrium adsorption of copper cyanide species onto activated carbon, *Hydrometallurgy*, 101, 99–107.
- Dai, X., Simons, A., Breuer, P. 2012. A review of copper cyanide recovery technologies for the cyanidation of copper containing gold ores, *Minerals Engineering*, 25, 1–13.
- Dash, R.R., Gaur, A., Balomajumder, C. 2009. Cyanide in industrial wastewaters and its removal: a review on biotreatment, *Journal of hazardous materials*, 163, 1–11.
- Donato, D.B., Madden-Hallett, D.M., Smith, G.B., Gursansky, W. 2017. Heap leach cyanide irrigation and risk to wildlife: Ramifications for the international cyanide management code, *Ecotoxicology and environmental safety*, 140, 271–278.
- Dunbar, K.R., Heintz, R.A. 1997. Chemistry of transition metal cyanide compounds: Modern perspectives, *Progress in Inorganic Chemistry*, 45, 283–392.
- Dwivedi, N., Balomajumder, C., Mondal, P. 2016. Comparative investigation on the removal of cyanide from aqueous solution using two different bioadsorbents, *Water Resources and Industry*, 15, 28–40.
- Eletta, O.A.A., Ajayi, O.A., Ogunleye, O.O., Akpan, I.C. 2016. Adsorption of cyanide from aqueous solution using calcinated eggshells: Equilibrium and optimisation studies, *Journal of Environmental Chemical Engineering*, 4, 1367–1375.
- Freundlich, H.M.F. 1906. Over the adsorption in solution, *The Journal of Physical Chemistry*, 57, 1100–1107.
- Gebresemati, M., Gabbiye, N., Sahu, O. 2017. Sorption of cyanide from aqueous medium by coffee husk: Response surface methodology, *Journal of Applied Research and Technology*, 15, 27–35.
- Guo, R., Chakrabarti, C.L., Subramanian, K.S., Ma, X., Lu, Y., Cheng, J., Pickering, W.F. 1993. Sorption of low levels of cyanide by granular activated carbon, *Water Environment Research*, 65, 640–644.
- Hadi, H.J., Al-zobai, K.M.M., Alatabe, M.J.A. 2020. Oil removal from produced water using imperata cylindrica as low-cost adsorbent, *Current Applied Science and Technology*, 494–511.
- Hattab, Z., Filali, N., Mazouz, R., Guerfi, K., Rebbani, N., Nafa, A., Kheriaf, S. 2016. Adsorption of cyanide ions in aqueous solution using raw and oxidized coke, *Desalination and Water Treatment*, 57, 3522–3531.
- Ho, Y.-S. 2006. Isotherms for the sorption of lead onto peat: comparison of linear and non-linear methods, *Polish Journal of Environmental Studies*, 15, 81–86.
- Ho, Y.-S., McKay, G. 1999. Pseudo-second order model for sorption processes, *Process Biochem.*, 34, 451–465.
- Ho, Y.-S., Ofomaja, A.E. 2006. Biosorption thermodynamics of cadmium on coconut copra meal as biosorbent, *Biochemical Engineering Journal*, 30, 117–123.
- Hussein, A.A., Alatabe, M.J.A. 2019. Remediation of Lead-Contaminated soil, using clean energy in combination with Electro-Kinetic methods, *Pollution*, 5, 859–869.
- Ibragimova, R.I., Grebennikov, S.F., Gur'yanov, V.V., Kubyshkin, S.A., Vorob'ev-Desyatovskii, N.V. 2013. Adsorption of $[\text{Au}(\text{CN})_2]^-$ ions from aqueous solutions on an activated carbon surface, *Protection of Metals and Physical Chemistry of Surfaces*, 49, 402–407.
- Jaafar, M., Alatabe, A. 2019. Utilization of low cost adsorbents for the adsorption process of lead ions, *International Journal of Modern Research in Engineering and Technology*, 4, 29–48.
- Kaewkannetra, P., Imai, T., Garcia-Garcia, F.J., Chiu, T.Y. 2009. Cyanide removal from cassava mill wastewater using *Azotobacter vinelandii* TISTR 1094 with mixed microorganisms in activated sludge treatment system, *Journal of hazardous materials*, 172, 224–228.
- Kalipci, E., Namal, O.O. 2018. Removal of Cr(VI) using a novel adsorbent modification. Ultrasonic method with apricot kernel shells, *Environment Protection Engineering*, 44, 79–92.

- Krasilnikova, O.K., Artamonova, S.D., Voloshchuk, A.M., Yevsyukhin, A.E. 2005. Production of carbonaceous adsorbents from apricot kernels, *Solid Fuel Chemistry*, 39, 57–62.
- Kulig, K.W, Ballantyne, B. 1991. Cyanide toxicity. Atlanta, GA: U.S. Dept. of Health & Human Services, Public Health Service, Agency for Toxic Substances and Disease Registry, Print.
- Kurama, H., Çatalsarik, T. 2000. Removal of zinc cyanide from a leach solution by an anionic ion-exchange resin, *Desalination*, 129, 1–6.
- Langmuir, I. 1916. The constitution and fundamental properties of solids and liquids. *Journal of the American Chemical Society*, 38, 2221–2295.
- Langmuir, I. 1917. The constitution and fundamental properties of solids and liquids. II. Liquids., *Journal of the American Chemical Society*, 39, 1848–1906.
- Langmuir, I. 1918. The adsorption of gases on plane surfaces of glass, mica and platinum., *Journal of the American Chemical Society*, 40, 1361–1403.
- Liu, Y. 2009. Is the free energy change of adsorption correctly calculated?, *Journal of Chemical & Engineering Data*, 54, 1981–1985.
- Lu, D., Chang, Y., Wang, W., Xie, F., Asselin, E., Dreisinger, D. 2015. Copper and cyanide extraction with emulsion liquid membrane with LIX 7950 as the mobile carrier: part 1, Emulsion stability, *Metals (Basel)*, 5, 2034–2047.
- Mbadcam, J.K., Ngomo, H.M., Tcheka, C., Rahman, A.N., Djoyo, H.S., Kouotou, D. 2009. Batch equilibrium adsorption of cyanides from aqueous solution onto copper-and nickel-impregnated powder activated carbon and clay, *Journal of Environmental Protection Science*, 3, 53–57.
- Meenakshi, S., Viswanathan, N. 2007. Identification of selective ion-exchange resin for fluoride sorption, *Journal of Colloid and Interface Science*, 308, 438–450.
- Namal, O.O., Kalipci, E. 2020. Adsorption kinetics of methylene blue removal from aqueous solutions using potassium hydroxide (KOH) modified apricot kernel shells, *International Journal of Environmental Analytical Chemistry*, 100, 1549–1565.
- Nourozi, R., NooriSepehr, M., Zarrabi, M. 2015. Adsorption of cyanide from aqueous solutions using magnetic hydroxyapatite nanoparticles synthesized by hydrothermal method: Equilibrium and kinetic study, *Journal of Health*, 5, 275–288.
- Pan, B., Xing, B. 2010. Adsorption kinetics of 17 α -ethinyl estradiol and bisphenol A on carbon nanomaterials. I. Several concerns regarding pseudo-first order and pseudo-second order models, *Journal of Soils and Sediments*, 10, 838–844.
- Papari, F., Sahebi, S., Kouhgardi, E., Behresi, R., Hashemi, S., Asgari, G., Jorfi, S., Ramavandi, B. 2017. Cyanide adsorption from aqueous solution using mesoporous zeolite modified by cetyltrimethylammonium bromide surfactant., *Desalination and Water Treatment*, 97, 285–294.
- Parga, J.R., Shukla, S.S., Carrillo-Pedroza, F.R. 2003. Destruction of cyanide waste solutions using chlorine dioxide, ozone and titania sol, *Waste Management*, 23, 183–191.
- Paschka, M.G., Ghosh, R.S., Dzombak, D.A. 1999. Potential water-quality effects from iron cyanide anticaking agents in road salt, *Water Environment Research*, 71, 1235–1239.
- Saleh, T.A., Siddiqui, M.N., Al-Arfaj, A.A. 2016. Kinetic and intraparticle diffusion studies of carbon nanotubes-titania for desulfurization of fuels, *Petroleum Science and Technology*, 34, 1468–1474.
- Sarma, G.K., Gupta, S.S., Bhattacharyya, K.G. 2019. Nanomaterials as versatile adsorbents for heavy metal ions in water: a review, *Environmental Science and Pollution Research*, 26, 6245–6278.
- Sheremata, T.W., Hawari, J. 2000. Mineralization of RDX by the white rot fungus *Phanerochaete chrysosporium* to carbon dioxide and nitrous oxide, *Environmental Science & Technology*, 34, 3384–3388.
- Simonin, J.-P., Bouté, J. 2016. Intraparticle diffusion-adsorption model to describe liquid/solid adsorption kinetics, *Revista mexicana de ingeniería química*, 15, 161–173.
- Sun, B., Long, Y., Chen, Z., Liu, S., Zhang, H., Zhang, J., Han, W. 2014. Recent advances in flexible and stretchable electronic devices via electrospinning, *Journal of Materials Chemistry C*, 2, 1209–1219.
- Vadi, M., Abbasi, M., Zakeri, M., Jafari, Y.B. 2011. Application of the Freundlich Langmuir Temkin and Harkins-Jura adsorption isotherms for some amino acids and amino acids complexation with manganese ion (II) on carbon nanotube, *International Conference on Nanotechnology and Biosensors IPCBEE vol.2 © (2011) IACSIT Press, Singapore*.
- Vadi, M., Abbasi, M., Zakeri, M., Yazdi, B.J. 2010. Application of the Freundlich Langmuir Temkin and Harkins-Jura adsorption isotherms for some amino acids and amino acids complexation with manganese kn(II) on carbon nanotube, *Journal of Physical & Theoretical Chemistry*, 7, 33–42.
- Wu, F.-C., Tseng, R.-L., Juang, R.-S. 2009. Characteristics of Elovich equation used for the analysis of adsorption kinetics in dye-chitosan systems, *Chemical Engineering Journal*, 150, 366–373.
- Xie, F., Wang, W. 2017. Recovery of copper and cyanide from waste cyanide solutions using emulsion liquid membrane with LIX 7950 as the carrier, *Environmental Technology*, 38, 1961–1968.
- Zhang, D., Ma, Y., Feng, H., Hao, Y. 2012. Adsorption of Cr (VI) from aqueous solution using carbon-microsilica composite adsorbent, *Journal of the Chilean Chemical Society*, 57, 964–968.
- Zhang, Q.-A., Wu, D.-D., Wei, C.-X. 2019. Purification of amygdalin from the concentrated Debitterizing-Water of apricot kernels using XDA-1 resin, *Processes*, 7, 359.